

10-2014

# HES-Mediated Repression of Pten in *Caenorhabditis elegans*

Han Ting Chou

*Georgia State University*, hchou2@gsu.edu

Raymarie Gomez Vazquez

*Georgia State University*, rgomezvazquez1@gsu.edu

Kun Wang

*New York University School of Medicine*, kwang4@student.gsu.edu

Richard Campbell

*Georgia State University*, rcampbell15@student.gsu.edu

Gaolin Zheng Milledge

*North Carolina Central University*

*See next page for additional authors*

Follow this and additional works at: [http://scholarworks.gsu.edu/biology\\_facpub](http://scholarworks.gsu.edu/biology_facpub)

 Part of the [Biology Commons](#)

---

## Recommended Citation

HES-Mediated Repression of Pten in *Caenorhabditis elegans* Han Ting Chou, Raymarie Gomez Vazquez, Kun Wang, Richard Campbell, Gaolin Zheng Milledge, Walter W. Walthall, and Casonya M. Johnson G3 December 2015 5:2619-2628; Early Online October 4, 2015, doi:<http://dx.doi.org/10.1534/g3.115.019463>

This Article is brought to you for free and open access by the Department of Biology at ScholarWorks @ Georgia State University. It has been accepted for inclusion in Biology Faculty Publications by an authorized administrator of ScholarWorks @ Georgia State University. For more information, please contact [scholarworks@gsu.edu](mailto:scholarworks@gsu.edu).

---

**Authors**

Han Ting Chou, Raymarie Gomez Vazquez, Kun Wang, Richard Campbell, Gaolin Zheng Milledge, Walter W. Walthall, and Casonya Matese Johnson

## HES-mediated Repression of Pten in *C. elegans*

Han Ting Chou<sup>\*§</sup>, Raymarie Gomez Vazquez<sup>\*</sup>, Kun Wang<sup>#</sup>, Richard Campbell<sup>\*</sup>, Gaolin Zheng Milledge<sup>‡</sup>, Walter W. Walthall<sup>\*</sup>, Casonya M. Johnson<sup>\*§</sup>

<sup>\*</sup>Department of Biology and <sup>§</sup>Center for Obesity Reversal, College of Arts and Sciences, Georgia State University, Atlanta, GA 30303, USA

<sup>#</sup>Department of Environmental Health Science, Division of Biostatistics, New York University School of Medicine, New York, NY 10016, USA

<sup>‡</sup>Department of Mathematics and Computer Science, North Carolina Central University, Durham, NC 27707, USA

**Running title:** HLH-25 enhances dauer recovery

**Keywords:** hairy/enhancer-of-split; dauer recovery; gonad morphology; unfertilized oocytes; gene expression microarray

**Corresponding Author:**

Casonya M. Johnson  
Georgia State University  
Department of Biology  
161 Jesse Hill Jr. Dr., SE  
Atlanta, GA 30303  
Phone: 404-413-5426  
Electronic mail: [cjohnson113@gsu.edu](mailto:cjohnson113@gsu.edu)



**ABSTRACT** The Hairy/Enhancer-of-Split (HES) group of transcription factors controls embryonic development, often by acting downstream of the Notch signaling pathway; however, little is known about postembryonic roles of these proteins. In *Caenorhabditis elegans*, the six proteins that make up the REF-1 family are considered to be HES orthologs that act in both Notch dependent and Notch-independent pathways to regulate embryonic events. To further our understanding of how the REF-1 family works to coordinate post-embryonic cellular events, we performed a functional characterization of the REF-1 family member, HLH-25. We show that, after embryogenesis, *hlh-25* expression persists throughout every developmental stage, including dauer, into adulthood. Like animals that carry loss-of-function alleles in genes required for normal cell cycle progression, the phenotypes of *hlh-25* animals include reduced brood size, unfertilized oocytes, and abnormal gonad morphology. Using gene expression microarray, we show that the HLH-25 transcriptional network correlates with the phenotypes of *hlh-25* animals, and that the *C. elegans* Pten ortholog, *daf-18*, is one major hub in the network. Finally, we show that HLH-25 regulates *C. elegans* lifespan and dauer recovery, which correlates with a role in the transcriptional repression of *daf-18* activity. Collectively, these data provide the first genetic evidence that HLH-25 may be a functional ortholog of mammalian HES1, which represses PTEN activity in mice and human cells.

## INTRODUCTION

In *Caenorhabditis elegans*, HLH-25 is one of six members of the REF-1 family of basic helix-loop-helix (bHLH) transcription factors (ALPER and KENYON 2001). This family is characterized by the presence of two bHLH domains, and are considered functional orthologs of the Hairy Enhancer of Split (HES) family, partly because of their roles as HES-like transducers of Notch signaling in early embryos (NEVES and PRIESS 2005). REF-1, the first family member to be identified via genetic screens, acts downstream of both Notch and GATA signaling to direct endoderm specification (HERMANN *et al.* 2000; NEVES *et al.* 2007) and to direct neuronal lineage decisions (LANJUN *et al.* 2006), including the V-ray lineage in *C. elegans* males (ROSS *et al.* 2005). In addition to acting downstream of embryonic Notch signaling events, the family member HLH-29 is targeted by LIN-12/Notch during vulva muscle formation in L4 stage animals (LI *et al.* 2013). HLH-29 also acts post-embryonically to transcriptionally regulate a diverse set of genes, including those required for chemorepulsive behaviors (MCMILLER *et al.* 2007), IP3-mediated

movement of unfertilized oocytes and fertilized eggs through the spermatheca (WHITE *et al.* 2012), iron homeostasis, and oxidative stress response (QUACH *et al.* 2013).

Biological roles have not yet been identified for HLH-25. Notch-dependent, embryonic expression of the gene *hlh-25* occurs in descendants of the AB blastomeres, cells that eventually give rise to the pharynx, the nervous system, and the hypodermis (NEVES and PRIESS 2005; SCHNABEL and PRIESS 1997). Notch-independent, embryonic expression of *hlh-25* is mediated by the GATA factor MED-1 and occurs in descendants of the MS blastomere, which also give rise to the pharynx and muscle and to the somatic gonad (BROITMAN-MADURO *et al.* 2005; SCHNABEL and PRIESS 1997). Yeast two-hybrid analysis and protein binding microarrays suggest that the REF-1 family proteins fail to heterodimerize with other bHLH proteins and instead bind E-box-like sequences as homodimers (GROVE *et al.* 2009; POWELL *et al.* 2004). Of all the REF-1 family proteins, HLH-25 has the highest degree of DNA-binding promiscuity and tightly binds to five E-box-like sequences. As a comparison, REF-1 binds tightly and HLH-26

binds weakly to the same E-box-like sequence, while HLH-29 only binds weakly to two sequences (GROVE *et al.* 2009). Gene ontology of the genes containing HLH-25 binding sites predicts that HLH-25 plays critical roles in cell division and development, including embryonic development, larval development, growth, and specification of cell fate (GROVE *et al.* 2009).

HLH-25's putative role in regulating cell division and embryonic and post-embryonic development supports earlier studies suggesting that the *C. elegans* REF-1 family proteins are orthologs of the mammalian HES protein family (NEVES *et al.* 2007). Like the other REF-1 family proteins, the sequence similarity between HLH-25 and the HES protein family lies within the bHLH domain. HLH-25 is more similar to HES1 than to the other mouse HES proteins, but is most similar to the mouse Atonal homolog protein Math1 when amino acid residues flanking the bHLH domain are included in the analysis. Both Atonal1 and Hes1 play well established roles in directing neuronal cell fate decisions (AKAZAWA *et al.* 1995; BEN-ARIE *et al.* 2000; OUJI *et al.* 2013; TOMITA *et al.* 2000; WANG *et al.* 2001), as do the respective, previously characterized *C. elegans* orthologs LIN-32 and LIN-22 (MILLER and PORTMAN 2011; WRISCHNIK and KENYON 1997). Other studies suggest that the human and mouse HES1 proteins are oncogenic (AXELSON 2004; GAO *et al.* 2014; SANG *et al.* 2010), underscoring the roles that these proteins play in regulating cell division and cell proliferation.

In this study, we describe a functional characterization of HLH-25 using reverse genetics and molecular approaches. We show that *hlh-25* is expressed post-embryonically in body wall muscles and in neurons, and that the phenotypes of *hlh-25* animals include reduced brood size, unfertilized oocytes, and abnormal gonad morphology, all of which are consistent with defective cell cycle or cell division events during embryogenesis. We

show that the predicted HLH-25 transcriptional network, based on gene expression microarray, includes the Pten ortholog DAF-18 and other genes that mediate cell division, embryonic development, and larval development. Finally, we show that the ability of HLH-25 to facilitate dauer recovery and lifespan correlates with our mRNA studies suggesting that HLH-25 transcriptionally represses *daf-18*/Pten expression.

## RESULTS

**Phenotypes of *hlh-25(ok1710)* animals and *Phlh-25::GFP* activity suggest roles for HLH-25 in reproduction.** Previous studies indicate that *hlh-25* is expressed in 8-cell stage embryos in response to Notch signalling, and in later stage embryos in response to GATA signalling (BROITMAN-MADURO *et al.* 2005; NEVES and PRIESS 2005). Using an *hlh-25::GFP* transcriptional reporter *cmjEx31* (Figure S1), we detected post-embryonic expression of *hlh-25* at all larval and adult stages, including dauer stage, in unidentified neurons of the head and tail, the anal depressor muscle, anterior and posterior intestinal cells, and the head and body wall muscles of transgenic animals (Figure 1). We detected expression in the PDE sensory neuron pairs and rare, transient expression in migrating distal tip cells of L3/L4 stage animals. We also detected stage-specific *hlh-25* expression in multiple neurons of the ventral nerve cord in starvation-induced dauer stage animals. We were able to use cell body location and commissure morphology to identify three of the motor neurons as VD1, DA3, and DA7. Expression in the body wall and head muscles and in the PDE neuron pair was not evident in dauer larvae.

The *hlh-25(ok1710)* allele is a null allele that was generated by EMS mutagenesis. It is a 1550 bp deletion that spans from 292 bp upstream of the initiator codon to 348 bp downstream of the terminator codon (Figure

S1). We outcrossed these animals 10 times, confirmed homozygosity for the *ok1710* allele by PCR, and then examined them for mutant phenotypes. *hlh-25(ok1710)* animals produced fewer live progeny at 20°C than wild-type animals (Figure 2A, P-value = 0.0027) while laying more unfertilized oocytes (P-value = 0.00014) throughout the egg-laying period.

Adult hermaphrodites produce more oocytes than sperm, and will continue to lay unfertilized eggs for a short period after depleting their sperm supply. Under conditions where food is plentiful, and when cultured at 20°C, wild-type hermaphrodites lay eggs over the first five days of adulthood (WARD and CARREL 1979; WHITE *et al.* 2012). As previously described, we found that wild-type animals lay an increasing number of unfertilized eggs as the sperm supply diminishes. In our assays, wild-type animals continued to lay a small number of unfertilized eggs for one additional day after the active egg-laying period ended (egg-laying day 6), to produce an average total of 49 unfertilized oocytes (Figure 2B, Table S1). *hlh-25(ok1710)* animals continued to produce unfertilized oocytes for four days after the active egg-laying period ended (egg-laying day 9), and produced an average total of 232 unfertilized oocytes. This phenotype has been recently named uno-o (RIESEN *et al.* 2014), and is also seen in animals that carry null alleles of the REF-1 family protein HLH-29 (WHITE *et al.* 2012). We were able to partially rescue the uno-o phenotype in *hlh-25(ok1710)* animals by expressing *hlh-25* from an extrachromosomal array, *cmjEx32*, so that transgenic animals produced an average of 38% fewer unfertilized oocytes than *hlh-25(ok1710)* animals (Figure 2A).

We also examined the gonad arms of adult hermaphrodites. In wild-type animals, oocytes production occurs as progressive movement through two U-shaped gonad arms, starting with the production of germline

nuclei at the distal end of each gonad arm, and ending with the ovulation of the oocyte into the sperm-filled spermatheca at the ends proximal to the uterus (HUBBARD and GREENSTEIN 2000). In the distal, syncytial region of each arm, the germline nuclei go through mitotic and meiotic divisions while being surrounded by a commonly shared cytoplasmic core. Nuclei start to compartmentalize into oocytes as they move progressively closer to a bend in the gonad arm, and are fully compartmentalized, or budded, as they leave the bend and proceed towards the spermatheca (GREEN *et al.* 2011). We found that organization of the gonad arm and germline progression were abnormal in 63% of *hlh-25(ok1710)* animals. As shown in Figure 3 and in Figures S2 and S3, gonad architecture was variably abnormal and included constrictions in the distal and proximal gonad arms, increased apoptosis, increased oocyte number, delayed oocyte compartmentalization, abnormal chromatin condensation, and arrested embryos in the uterus.

Other phenotypes of *hlh-25(ok1710)* animals included decreased movement as monitored by thrashing and locomotion assays (Figure S4), leading us to classify *hlh-25* mutants as locomotion variants. This phenotype correlates with the expression of *cmjEx31* in the body wall muscles and in head neurons, but we could not accurately assay for rescue of this phenotype by transgenic expression of *hlh-25* because transgenic animals also carried the *rol-6* marker, which causes a dominant locomotor defect. We did not pursue the locomotion phenotype further in this study.

**DAF-18 is one major hub in the *hlh-25* transcriptional network.** We used gene expression microarray to compare the expression profiles of late L4/young-adult stage *hlh-25(ok1710)* animals to profiles of age-matched, wild-type animals. We found

that the expression of 630 genes, 506 of which were up-regulated and 124 of which were down-regulated, was altered by at least 2.0 fold (Table S2), and confirmed by RT-qPCR that the expression of 21 genes was significantly affected in L4-stage *hlh-25(ok1710)* animals (Table 1). As shown in Table 1, the direction of the change in expression was the same for 18 of the 21 genes. It is possible that the opposite, but significant change in the three remaining genes was due to differences in the developmental age of animals at the times of RNA extraction. Interestingly, 152 of these genes, indicated by asterisks in Tables 1 and S2, contain predicted HLH-25 binding sites within their putative promoters (GROVE *et al.* 2009). Hypergeometric analysis, indicated that this overlap of 152 genes was significantly lower than expected when compared to an overlap between the list of genes identified by protein binding microarray to a randomly chosen gene set of the same size (P-value  $<2.5 \times 10^{-05}$ ).

We clustered related target genes based on enriched gene ontology (GO) terms. A total of 328 genes were organized into 10 annotation clusters that all fit within the broad category of 'Development' (top eight clusters are shown in Figure 4A). Using the Search Tool for the Retrieval of Interacting Genes/Proteins (STRING 9.0) to identify predicted and known interactions between proteins encoded by the target genes (SZKLARCZYK *et al.* 2011), we found that the *hlh-25* regulatory network has a high degree of overlap and interconnectivity. For example, 38 genes clustered under the GO term 'SEXUAL REPRODUCTION.' Of those, 22 genes (58%) formed a single, highly interconnected, interaction network (Figure 4B) and were also associated with at least two other clusters. This trend of high connectivity among genes within a cluster and significant overlap among genes between clusters was evident for the entire network. We also identified six genes

that we considered to be major hubs (Table 2). These genes were associated with at least four of the GO clusters and formed predicted interactions with at least 35 other targets in the network. Importantly, the hub genes underscore the developmental influence of the *hlh-25* regulatory network, encoding helicases, cyclins, and RNA binding proteins with established roles in embryogenesis (Table 2). The *C. elegans* homolog of the mammalian *Pten* tumor suppressor, DAF-18 (MASSE *et al.* 2005), is one of the major hubs, forming connections with 62 proteins distributed across six annotation clusters (Figure 4C, bold genes in Table S2).

**HLH-25 functions upstream of DAF-18 to regulate dauer recovery.** It is not clear whether the REF-1 proteins and the HES proteins arose from the same parent gene; however, conservation within the helix-loop-helix domains and the ability to transduce Notch signals suggest that REF-1 proteins and HES proteins are members of the same functional family. Importantly, the identification of *daf-18* as a major hub in the HLH-25 transcriptional network, together with the identification of predicted HLH-25 binding sites in the *daf-18* promoter (GROVE *et al.* 2009), underscores the functional homology between the HLH-25 and vertebrate HES1 protein. In the mouse thymus, HES1 acts downstream of Notch signalling to repress *Pten* activity during T-cell differentiation (WONG *et al.* 2012), and the resistance of T-cell acute lymphoblastic leukemia (T-ALL) cells to Notch inhibition depends on functional HES1 binding sites in the *Pten* promoter (PALOMERO *et al.* 2007). Therefore, we further characterized the genetic interaction between the genes encoding the HES homolog HLH-25 and the PTEN homolog DAF-18.

Using RT-qPCR we found that the levels of *daf-18* mRNA increase greater than 2-fold in embryos (data not shown) and in L4 stage animals (Table 1) compared to age-

matched controls. The levels of *daf-18* mRNA also increased in wild-type animals that were subjected to *hlh-25* RNAi (Figure S5), suggesting that the increased *daf-18* activity is due to loss of HLH-25 in *hlh-25(ok1710)* animals. We failed to detect differences in *daf-18* transcriptional activity in wild-type and *hlh-25* animals expressing *Pdaf-18::GFP* via a previously described, integrated transgene. These animals were generated in a *daf-2* loss-of-function background, which increases the transcriptional activity of the *daf-18* promoter (SOLARI *et al.* 2005). It is possible that loss of *daf-2* masks the effects of HLH-25. Unfortunately, we have not yet been successful in generating stably transgenic lines expressing *Pdaf-18::GFP* in animals that produce functional DAF-2.

In *C. elegans*, longevity and entry into dauer stage are controlled through the insulin signalling pathway, and depend on the insulin receptor DAF-2. Decreased insulin signalling, via loss-of-function mutations in *daf-2*, increases *C. elegans* lifespan and causes a dauer-constitutive phenotype. These phenotypes are suppressed in *daf-18* animals: *daf-18* animals have reduced lifespan (SOLARI *et al.* 2005) and animals that carry strong loss-of-function alleles are unable to undergo dauer development (GIL *et al.* 1999; MIHAYLOVA *et al.* 1999; ROUAULT *et al.* 1999). The reduced lifespan of *daf-18* animals can be rescued, and slightly extended beyond the wild-type lifespan, by the overexpression of *daf-18* from the extra-chromosomal array *quls18* (BRISBIN *et al.* 2009; SOLARI *et al.* 2005). We reasoned that since *hlh-25(ok1710)* animals have increased *daf-18* activity, they should have an extended lifespan. As expected, the lifespan of *hlh-25(ok1710)* animals (median LS = 19 days) is significantly longer than the lifespan of wild-type animals (median LS = 16 days, P-value <0.0001) grown at 20°C (Figure 5A). This result is comparable to the extended lifespan

previously reported for *C. elegans quls18* females (BRISBIN *et al.* 2009).

Normally when wild-type, starvation-induced dauer larvae are moved to favorable growth conditions, they take approximately 60 minutes to commit to exiting the dauer stage at 25°C, and they molt into the L4 stage at approximately ten hours (GOLDEN and RIDDLE 1982; GOLDEN and RIDDLE 1984a; GOLDEN and RIDDLE 1984b; GOLDEN and RIDDLE 1984c). As animals begin to exit dauer stage and enter into the L4 molt, fat accumulation and pharyngeal pumping begin after approximately 60 minutes and three hours, respectively, of making the dauer recovery/exit decision (PROUDFOOT *et al.* 1993). The onset of vulva formation is detectable within twelve hours of the exit decision, and recovering dauers enter late L4/early adult stage within 24 hours of the decision to exit dauer stage.

Because *daf-18(ok480)* do not form dauers under starvation conditions, we used heat stress to induce dauer formation via an IIS-independent pathway in wild-type, *hlh-25(ok1710)*, *daf-18(ok480)*, and *quls18* animals, and compared their dauer recovery phenotypes. We found that at least 80% of wild-type animals (n = 1199) reached early L4 stage within 12 hours after the switch to 20°C. As expected, dauer recovery was similar to wild-type in *daf-18(ok480)* animals (n = 485) but was longer in *quls18* animals (n = 955). At 12 hours, approximately 65% of the *daf-18(ok480)* animals, but only 10% of the *quls18* animals, reached early L4. Interestingly, the dauer recovery timing of the *hlh-25(ok1710)* animals (n = 738) was very similar to the *quls18* animals: only 21% of *hlh-25(ok1710)* animals reached L4 stage within 12 hours, and only 45% reached L4 stage within 24 hours. This delayed dauer recovery phenotype in *hlh-25(ok1710)* animals was partially rescued by transgenic expression of *hlh-25 (cmjEx32)*: 70% of transgenic animals (n = 300) reached L4 within 24 hours. For a more quantitative



approach, we monitored the onset of pharyngeal pumping during dauer recovery. Dauer recovery in *daf-18(ok480)* animals was not significantly different from recovery in wild-type animals; however, it took 1.5 times longer for the onset of pharyngeal pumping to occur in 50% of *hlh-25(ok1710)* animals (P-value <0.0001) than in wild-type animals (Figure 5B). This delay was rescued by transgenic expression of *hlh-25* (Figure 5C). These results, together with our gene expression data, suggest that HLH-25 acts upstream of *daf-18* to negatively regulate lifespan and dauer recovery.

## DISCUSSION

This study is a functional characterization of HLH-25, a member of the *C. elegans* REF-1 family of transcriptional regulators. Previous studies have shown that the gene *hlh-25* is transcriptionally activated through Notch-signaling in cells that eventually give rise to the pharynx and nervous system, and through the Notch-independent GATA family of transcription factors in tissues that give rise to the pharynx, muscle, and somatic gonad. Here we show that expression of *hlh-25* persists throughout the *C. elegans* life cycle. Although we identified a number of HLH-25 targets that are germline expressed and whose mRNAs are stored in oocytes prior to fertilization, we were unable to recover transgenic lines that report germline expression of *hlh-25*. Future studies may further define the role of HLH-25 in embryogenesis, which includes determining whether the maternal contribution of HLH-25 is required for proper embryogenesis.

Our results show that the phenotypes of *hlh-25* animals include reduced brood size, unfertilized oocytes in the uterus, abnormal gonad morphology/architecture, extended lifespan, and delayed dauer recovery. In previous studies, functional annotation of candidate target genes suggested overlapping

roles in cell signaling events for all of the REF-1 family proteins, and HES-like roles for HLH-25 and HLH-29 in regulating embryonic and larval development, growth, cell fate specification, and reproductive behaviors (GROVE *et al.* 2009). Interestingly, this functional overlap is suggested, but not clearly evident, in the phenotypes of REF-1 family mutants that have been characterized to date. Both *ref-1* and *hlh-29* animals, for example, show varying degrees of embryonic lethality that would ultimately lead to reduced brood size (ALPER and KENYON 2001; McMILLER *et al.* 2007; WHITE *et al.* 2012); however the reduced brood size in *hlh-25* animals is not due to lethality during embryogenesis, but to abnormalities that occur prior to fertilization. Likewise, mutations in *ref-1*, *hlh-29*, and *hlh-25* cause morphological defects that affect sexual reproduction. Loss of *ref-1* affects cell fusion events during vulva morphogenesis (ALPER and KENYON 2001) and ray lineage decisions during morphogenesis of the male tail (ROSS *et al.* 2005). Loss of either *hlh-29* or *hlh-25* results in unfertilized oocytes, abnormal gonad morphologies, and the exploded through vulva phenotype; however, the underlying mechanisms of these phenotypes appears to differ in *hlh-25* and *hlh-29* animals. The unfertilized oocyte phenotype in *hlh-29* animals, for example, is caused in part by altered expression of genes required for inositol 1, 4, 5-triphosphate (IP<sub>3</sub>) signaling, which affects the ability of oocytes and eggs to move through the spermatheca (WHITE *et al.* 2012). Based on our observations of independent ovulation events, however, spermatheca function in *hlh-25* animals appears normal, and genes required for IP<sub>3</sub> signaling are not affected by loss of HLH-25. These data suggest that the REF-1 family proteins do not act within a single transcriptional cascade to regulate specific events, and that each family member plays unique, stage-specific roles in *C. elegans* development.

Our gene expression microarray analysis suggests that there are six major hubs in the HLH-25 transcriptional network, including the *C. elegans* PTEN homolog, *daf-18*. We demonstrated by RT-qPCR that *daf-18* expression is normally repressed by HLH-25. This result is the first direct correlation between a HES protein target gene in mammals and a REF-1 family target gene in *C. elegans*. Hes1 directs cell division, in part, by repressing *Pten* expression in mouse (WONG *et al.* 2012), in human large cell neuroendocrine carcinoma (NASGASHIO *et al.* 2011), and in regenerating Clara cells of wild-type lungs (XING *et al.* 2012). In *C. elegans*, DAF-18 is required during embryogenesis to maintain G2 arrest in germline precursor cells (FUKUYAMA *et al.* 2006) via inhibition of Tor complex 1 signaling (FUKUYAMA *et al.* 2012). We did not examine embryonic or L1-stage phenotypes of *hlh-25* animals; however, we show that, like animals that overexpress *daf-18* (BRISBIN *et al.* 2009; LIU and CHIN-SANG 2015), *hlh-25* animals have an extended lifespan and take longer to exit dauer stage. Further examination of both the embryonic and post-embryonic regulation of *daf-18* by HLH-25 will further our understanding of the mechanisms and biological significance of HES-dependent activation and repression of PTEN.

*C. elegans* enter the dauer stage in response to adverse growth conditions, maintain this state while conditions remain undesirable, and then exit, or recover from dauer stage when environmental conditions are more favorable (HU 2007; OUELLET *et al.* 2008). The decision and ability to enter into dauer stage requires the integration of dietary and environmental signals through multiple molecular pathways, including insulin/IGF, TGF- $\beta$ , and guanylyl cyclase, and the molecular details of dauer entry in response to starvation, heat stress, and overcrowding have been well established (reviewed in FIELENBACH and ANTEBI 2008). Less is known

about the molecular requirements for dauer maintenance and dauer recovery. Studies suggest that GLP-1 dependent Notch activation in chemosensory neurons is required for dauer maintenance (OUELLET *et al.* 2008), and that metabotropic acetylcholine signaling is required for the induction of an insulin-like signal during dauer recovery (TISSENBAUM *et al.* 2000). Previous studies have also shown that dauer recovery requires LIN-12 dependent Notch activation, though the downstream target of this signaling event has not been identified (OUELLET *et al.* 2008). Future studies will determine whether HLH-25 acts downstream of Notch to modulate dauer recovery by repressing *daf-18* activity.

Finally, gene ontology and protein interaction analysis of the HLH-25 network suggests that HLH-25 affects genes required for three highly connected processes: cell division, cell cycle regulation, and reproduction, including gamete formation. The connectivity between the genes in these processes suggests that the HLH-25 regulatory network is amendable to change without the corresponding disruption in overall functionality. This feature is illustrated by the hub gene *daf-18*, and the hub genes *cgh-1*, *cyb-2.1*, *cyb-3*, *mcm-3*, and *puf-3*, which encode proteins required for early embryonic cytokinesis, meiosis II, G2/mitosis transition, licensing of DNA replication, and spindle positioning, respectively (AUDHYA *et al.* 2005; BOAG *et al.* 2005; HUBSTENBERGER *et al.* 2012; KAITNA *et al.* 2002; SONNEVILLE *et al.* 2012; VAN DER VOET *et al.* 2009). Though mutations in any of the hub genes, or in any of the nodes connected to them, result in severe phenotypes, including sterility, mutant animals are viable and have functional cell cycles. Future work will include further defining and validating the HLH-25 transcriptional network and correlating this network with the post-embryonic functions of HLH-25.

Taken together, our results demonstrate that the *C. elegans* HES

homolog, HLH-25, functions post-embryonically to transcriptionally regulate genes required for cell division, cell cycle regulation, and sexual reproduction, including the gene encoding the *C. elegans* Pten homolog, DAF-18.

## MATERIALS AND METHODS

### ***C. elegans* Growth and Culture Conditions**

The following strains were used: **N2** Bristol wild-type (BRENNER 1974); **VC1220**, *hlh-25(ok1710)* II; **RB712**, *daf-18(ok480)* IV; **IC748**, *qulS18*; **CMJ3001**, *cmjEX31(Phlh-25::GFP::unc-54'UTR in pPD95.67 + pRF4)*; **CMJ3002**, *hlh-25(ok1710)* II; *cmjEx32[(Phlh-25::hlh-25) + (Pmyo2::mCherry::unc-54'3'UTR)]*; and **CMJ3003**, *hlh-25(ok1710)* II; *daf-18(ok480)*. The extrachromosomal array *cmjEx31* includes 1540 nucleotides upstream of the predicted initiation codon, plus the first 30 nucleotides of the coding region for *hlh-25*, fused in-frame to sequences coding GFP. The extrachromosomal array *cmjEx32* includes the genomic DNA sequences spanning from 1540 nucleotides upstream of the initiator codon to 573 nucleotides downstream of the predicted stop codon for *hlh-25*. VC1220 animals were outcrossed 10 times to N2 animals, and final homozygosity was confirmed by PCR. Animals were maintained at 20°C on NGM agar plates seeded with *Escherichia coli* strain OP50 and were synchronized by alkaline hypochlorite treatment as previously described (LEWIS and FLEMING 1995). Bacteria mediated RNAi was performed as previously described (KAMATH *et al.* 2003; QUACH *et al.* 2013) using HT115 producing dsRNA for either the control gene *unc-55* or for *hlh-25/hlh-27*. The genes *hlh-25* and *hlh-27* are predicted to produce identical mRNAs and it is impossible to selectively silence *hlh-25*.

### **Microscopy**

For imaging, animals were anesthetized either with 0.2% levamisole (GOVINDAN *et al.* 2009) or with 10 mM NaN<sub>3</sub>, mounted on 2% agarose pads containing 10 mM NaN<sub>3</sub>, and imaged using either a 40X or a 60X water-immersion objective with the Nikon Eclipse 90i microscope equipped with a Nikon Coolsnap CCD camera. Z projections (sums of intensity) were obtained using NIS-Elements AR, version 4.0. For expression profiling, animals were cultured for at least 2 generations at 16°C and then were synchronized and allowed to grow to the appropriate stage (L1 to L4). Forty animals per larval stage were examined for expression. For dauer stage expression, 10 starvation-induced dauer were imaged.

### **Egg Laying Assays**

L4-stage animals were selected to individual NGM plates and allowed to molt to adulthood at 20°C. At the start of the egg laying period, each animal was moved daily to a new plate, already seeded with OP50, until 3 days after eggs or unfertilized oocytes were no longer detected. Eggs and oocytes were counted on the day that the hermaphrodite was removed. The plate was then incubated at 20°C for 24 hours, and the numbers of live progeny and unhatched eggs were counted. Eggs that did not hatch within the 24 hour period were scored as dead, while the number of live progeny was checked again in the next 24 hours and then removed. For rescue assays, the ratio of unfertilized oocytes to fertilized eggs was calculated daily.

### **Lifespan Assays**

Lifespan assays were performed as previously reported (QUACH *et al.* 2013). Lifespan survival comparisons were done individually for each of three biological replicates using the log rank test in GraphPad Prism 6 (GraphPad Software, Inc) and were then repeated with the data from all biological replicates combined into one experiment. Combined data are presented here.



### **Dauer Recovery Assays**

To induce dauer formation, embryos were collected by hypochlorite treatment, washed extensively in water, and then approximately 200 embryos were placed onto an NGM plate containing a sparse lawn of OP50 (~10  $\mu$ L of saturated OP50, 24 hours before use). Embryos were allowed to hatch, and the dauer larva to develop, undisturbed at 27°C for at least 96 hours. Cultures were visually examined to ensure that at least 90% of the larvae were arrested as dauer. Failure to include OP50 on the plate resulted in animals that arrested as starved L1 stage larvae. For dauer recovery, 25 dauers per strain were individually moved to a plate with a thick lawn of OP50 and incubated at 20°C. Dauers were examined every three hours over a twenty-four hour period for fat accumulation, pharyngeal pumping, crescent formation, and then at 8 hour intervals for another 24 hours for oocyte/embryo formation, and onset of egg-laying. The rates of onset of pharyngeal pumping were plotted as survival from dauer, and were compared by log-rank test using GraphPad Prism 6. The timing of dauer recovery varied with the day of the assay, with the onset of pumping occurring in 50% of wild-type animals as early as 3 hours or as late as 8.5 hours. In all assays the trend was the same, and the data shown are representative of one experiment.

### **Total RNA Isolation, cDNA Synthesis, Reverse Transcription, and Quantitative PCR**

Total RNA extraction and cDNA synthesis were carried out as previously described (QUACH *et al.* 2013) except total RNA was extracted from synchronized L4 stage animals. After cDNA synthesis, qPCR assays were performed with Taqman Gene Expression Assays (Invitrogen) for detection of amplicon, using relative quantitation with normalization against the endogenous control

gene *pmp-3* (HOOGEWIJS *et al.* 2008). Values shown represent the averages of at least three different experiments. The ID numbers for the Taqman Assays used in this study are available upon request.

### **Gene Expression Microarray**

Gene expression microarray (GEO Accession #GSE65417), including probe preparation, hybridization, fluidics run and chip scan, was performed by Georgia State University DNA/Protein Core Facility. Global gene expression in synchronized populations of VC1220 animals was compared to expression in N2 (wild-type) animals using GeneChip *C. elegans* Genome Array (Affymetrix). Data collection was carried out using GCOS 1.4 software (Affymetrix). Data analysis was performed using GeneSpring GX 11 Software (Agilent, Palo Alto, CA), and probe intensity values were normalized using Robust Multichip Average (RMA)-algorithm. The quality controls on samples and on probe sets were performed stepwise to detect the outlying samples and the poor probe sets. The Principal Components Analysis (PCA) score plot and hybridization controls plot were applied for sample detection. Those probe sets passing minimal detection cutoffs and quality control measurements subsequently were used for statistical analysis. The student's t-test was performed to find the candidates for differential expression, and genes with significant signal level between different conditions ( $p < 0.05$ ) were collected. In addition, fold change analysis were performed on the genes with significant expression, and all genes showing greater than two-fold change were considered putative targets.

### **Functional Analysis by Gene Ontology**

Gene Ontology (GO) analysis was performed using the Database for Annotation, Visualization and Integrated Discovery (DAVID), version 6.7, to cluster related target genes (HUANG DA *et al.* 2009a; HUANG DA *et al.*

2009b). Additional GO terms and functional information for putative targets were assigned based on Wormbase annotations (HARRIS *et al.* 2010). Interactions and connectivity between target gene products were identified using the Search Tool for the Retrieval of Interacting Genes/Proteins (SZKLARCZYK *et al.* 2011) and redrawn manually.

### Mobility Assays

For locomotion assays, individual L4 stage animals were placed by platinum wire onto an unseeded NGM plate, allowed to recover for 5 minutes, and then examined after the start of forward locomotion for 30-seconds. For thrashing assays, individual animals were placed into 50  $\mu$ L of M9 medium. Each lateral movement of the head was counted as one thrash, and movement was monitored for one 30 second interval per animal. Each biological replica included at least 25 animals per strain, and each assay was repeated for three biological replicas.

### ACKNOWLEDGEMENTS

We gratefully acknowledge our undergraduate research assistants, Emma Blasingame and Thai Tran for help with assays for brood size and embryonic viability, and the technical assistance of the Georgia State University microarray facility coordinator, Ms. Sonja Young. *Caenorhabditis elegans* strains used in this study were provided by the Caenorhabditis Genetics Center (funded by the NIH National Center for Research Resources, USA), Dr. I.D. Chin-Sang (Queens University), and Dr. F. Solari (Claude Bernard University). Portions of this work served to partially fulfill the requirements for the Masters of Science degree for R. Gomez Vazquez and K. Wang. The National Science Foundation grants MCB0919413 and MCB1139184 to C. Johnson supported this research and HT Chou, and provided stipend support for K. Wang and R. Gomez Vazquez, respectively.

R. Campbell is a GSU Brains and Behavior Fellow.

### REFERENCES

- AKAZAWA, C., M. ISHIBASHI, C. SHIMIZU, S. NAKANISHI and R. KAGEYAMA, 1995 A mammalian helix-loop-helix factor structurally related to the product of *Drosophila* proneural gene *atonal* is a positive transcriptional regulator expressed in the developing nervous system. *The Journal of biological chemistry* **270**: 8730-8738.
- ALPER, S., and C. KENYON, 2001 REF-1, a protein with two bHLH domains, alters the pattern of cell fusion in *C. elegans* by regulating Hox protein activity. *Development* **128**: 1793-1804.
- AUDHYA, A., F. HYNDMAN, I. X. MCLEOD, A. S. MADDOX, J. R. YATES, 3RD *et al.*, 2005 A complex containing the Sm protein CAR-1 and the RNA helicase CGH-1 is required for embryonic cytokinesis in *Caenorhabditis elegans*. *The Journal of cell biology* **171**: 267-279.
- AXELSON, H., 2004 The Notch signaling cascade in neuroblastoma: role of the basic helix-loop-helix proteins HASH-1 and HES-1. *Cancer letters* **204**: 171-178.
- BEN-ARIE, N., B. A. HASSAN, N. A. BIRMINGHAM, D. M. MALICKI, D. ARMSTRONG *et al.*, 2000 Functional conservation of *atonal* and *Math1* in the CNS and PNS. *Development* **127**: 1039-1048.
- BOAG, P. R., A. NAKAMURA and T. K. BLACKWELL, 2005 A conserved RNA-protein complex component involved in physiological germline apoptosis regulation in *C. elegans*. *Development* **132**: 4975-4986.
- BRENNER, S., 1974 The genetics of *Caenorhabditis elegans*. *Genetics* **77**: 71-94.
- BRISBIN, S., J. LIU, J. BOUDREAU, J. PENG, M. EVANGELISTA *et al.*, 2009 A role for C.

- C. elegans* Eph RTK signaling in PTEN regulation. *Developmental cell* **17**: 459-469.
- BROITMAN-MADURO, G., M. F. MADURO and J. H. ROTHMAN, 2005 The noncanonical binding site of the MED-1 GATA factor defines differentially regulated target genes in the *C. elegans* mesendoderm. *Dev Cell* **8**: 427-433.
- FIELNBACH, N., and A. ANTEBI, 2008 *C. elegans* dauer formation and the molecular basis of plasticity. *Genes Dev* **22**: 2149-2165.
- FUKUYAMA, M., A. E. ROUGVIE and J. H. ROTHMAN, 2006 *C. elegans* DAF-18/PTEN mediates nutrient-dependent arrest of cell cycle and growth in the germline. *Current biology : CB* **16**: 773-779.
- FUKUYAMA, M., K. SAKUMA, R. PARK, H. KASUGA, R. NAGAYA *et al.*, 2012 *C. elegans* AMPKs promote survival and arrest germline development during nutrient stress. *Biology open* **1**: 929-936.
- GAO, F., Y. ZHANG, S. WANG, Y. LIU, L. ZHENG *et al.*, 2014 Hes1 is involved in the self-renewal and tumorigenicity of stem-like cancer cells in colon cancer. *Scientific reports* **4**: 3963.
- GIL, E. B., E. MALONE LINK, L. X. LIU, C. D. JOHNSON and J. A. LEES, 1999 Regulation of the insulin-like developmental pathway of *Caenorhabditis elegans* by a homolog of the PTEN tumor suppressor gene. *Proceedings of the National Academy of Sciences of the United States of America* **96**: 2925-2930.
- GOLDEN, J. W., and D. L. RIDDLE, 1982 A pheromone influences larval development in the nematode *Caenorhabditis elegans*. *Science* **218**: 578-580.
- GOLDEN, J. W., and D. L. RIDDLE, 1984a A *Caenorhabditis elegans* dauer-inducing pheromone and an antagonistic component of the food supply. *Journal of chemical ecology* **10**: 1265-1280.
- GOLDEN, J. W., and D. L. RIDDLE, 1984b The *Caenorhabditis elegans* dauer larva: developmental effects of pheromone, food, and temperature. *Developmental biology* **102**: 368-378.
- GOLDEN, J. W., and D. L. RIDDLE, 1984c A pheromone-induced developmental switch in *Caenorhabditis elegans*: Temperature-sensitive mutants reveal a wild-type temperature-dependent process. *Proceedings of the National Academy of Sciences of the United States of America* **81**: 819-823.
- GOVINDAN, J. A., S. NADARAJAN, S. KIM, T. A. STARICH and D. GREENSTEIN, 2009 Somatic cAMP signaling regulates MSP-dependent oocyte growth and meiotic maturation in *C. elegans*. *Development* **136**: 2211-2221.
- GREEN, R. A., H. L. KAO, A. AUDHYA, S. ARUR, J. R. MAYERS *et al.*, 2011 A high-resolution *C. elegans* essential gene network based on phenotypic profiling of a complex tissue. *Cell* **145**: 470-482.
- GROVE, C. A., F. DE MASI, M. I. BARRASA, D. E. NEWBURGER, M. J. ALKEMA *et al.*, 2009 A multiparameter network reveals extensive divergence between *C. elegans* bHLH transcription factors. *Cell* **138**: 314-327.
- HARRIS, T. W., I. ANTOSHECHKIN, T. BIERI, D. BLASAR, J. CHAN *et al.*, 2010 WormBase: a comprehensive resource for nematode research. *Nucleic acids research* **38**: D463-467.
- HERMANN, G. J., B. LEUNG and J. R. PRIESS, 2000 Left-right asymmetry in *C. elegans* intestine organogenesis involves a LIN-12/Notch signaling pathway. *Development* **127**: 3429-3440.
- HOOGWIJS, D., K. HOUTHOOFD, F. MATTHIJSSSENS, J. VANDESOMPELE and J. R. VANFLETEREN, 2008 Selection and validation of a set of reliable reference genes for quantitative sod gene expression analysis in *C. elegans*. *BMC molecular biology* **9**: 9.

- HU, P. J., 2007 Dauer. WormBook: 1-19.
- HUANG DA, W., B. T. SHERMAN and R. A. LEMPICKI, 2009a Bioinformatics enrichment tools: paths toward the comprehensive functional analysis of large gene lists. *Nucleic acids research* **37**: 1-13.
- HUANG DA, W., B. T. SHERMAN and R. A. LEMPICKI, 2009b Systematic and integrative analysis of large gene lists using DAVID bioinformatics resources. *Nature protocols* **4**: 44-57.
- HUBBARD, E. J., and D. GREENSTEIN, 2000 The *Caenorhabditis elegans* gonad: a test tube for cell and developmental biology. *Dev Dyn* **218**: 2-22.
- HUBSTENBERGER, A., C. CAMERON, R. SHTOFMAN, S. GUTMAN and T. C. EVANS, 2012 A network of PUF proteins and Ras signaling promote mRNA repression and oogenesis in *C. elegans*. *Developmental biology* **366**: 218-231.
- KAITNA, S., H. SCHNABEL, R. SCHNABEL, A. A. HYMAN and M. GLOTZER, 2002 A ubiquitin C-terminal hydrolase is required to maintain osmotic balance and execute actin-dependent processes in the early *C. elegans* embryo. *Journal of cell science* **115**: 2293-2302.
- KAMATH, R. S., A. G. FRASER, Y. DONG, G. POULIN, R. DURBIN *et al.*, 2003 Systematic functional analysis of the *Caenorhabditis elegans* genome using RNAi. *Nature* **421**: 231-237.
- LANJUN, A., J. CLAGGETT, M. SHIBUYA, C. P. HUNTER and P. SENGUPTA, 2006 Regulation of neuronal lineage decisions by the HES-related bHLH protein REF-1. *Dev Biol* **290**: 139-151.
- LEWIS, J. A., and J. T. FLEMING, 1995 Basic culture methods. *Methods Cell Biol* **48**: 3-29.
- LI, P., K. M. COLLINS, M. R. KOELLE and K. SHEN, 2013 LIN-12/Notch signaling instructs postsynaptic muscle arm development by regulating UNC-40/DCC and MADD-2 in *Caenorhabditis elegans*. *eLife* **2**: e00378.
- LIU, J., and I. D. CHIN-SANG, 2015 *C. elegans* as a model to study PTEN's regulation and function. *Methods* **77-78**: 180-190.
- MASSE, I., L. MOLIN, M. BILLAUD and F. SOLARI, 2005 Lifespan and dauer regulation by tissue-specific activities of *Caenorhabditis elegans* DAF-18. *Developmental biology* **286**: 91-101.
- MCMILLER, T. L., D. SIMS, T. LEE, T. WILLIAMS and C. M. JOHNSON, 2007 Molecular characterization of the *Caenorhabditis elegans* REF-1 family member, hlh-29/hlh-28. *Biochim Biophys Acta* **1769**: 5-19.
- MIHAYLOVA, V. T., C. Z. BORLAND, L. MANJARREZ, M. J. STERN and H. SUN, 1999 The PTEN tumor suppressor homolog in *Caenorhabditis elegans* regulates longevity and dauer formation in an insulin receptor-like signaling pathway. *Proc Natl Acad Sci U S A* **96**: 7427-7432.
- MILLER, R. M., and D. S. PORTMAN, 2011 The Wnt/beta-catenin asymmetry pathway patterns the atonal ortholog lin-32 to diversify cell fate in a *Caenorhabditis elegans* sensory lineage. *The Journal of neuroscience : the official journal of the Society for Neuroscience* **31**: 13281-13291.
- NASGASHIO, R., Y. SATO, T. MATSUMOTO, T. KAGEYAMA, M. HATTORI *et al.*, 2011 The balance between the expressions of HASH1 and HES1 differs between large cell neuroendocrine carcinoma and small cell carcinoma of the lung. *Lung cancer* **74**: 405-410.
- NEVES, A., K. ENGLISH and J. R. PRIESS, 2007 Notch-GATA synergy promotes endoderm-specific expression of ref-1 in *C. elegans*. *Development* **134**: 4459-4468.
- NEVES, A., and J. R. PRIESS, 2005 The REF-1 family of bHLH transcription factors pattern *C. elegans* embryos through

- Notch-dependent and Notch-independent pathways. *Dev Cell* **8**: 867-879.
- OUELLET, J., S. LI and R. ROY, 2008 Notch signalling is required for both dauer maintenance and recovery in *C. elegans*. *Development* **135**: 2583-2592.
- OUI, Y., S. ISHIZAKA, F. NAKAMURA-UCHIYAMA, A. WANAKA and M. YOSHIKAWA, 2013 Induction of inner ear hair cell-like cells from Math1-transfected mouse ES cells. *Cell death & disease* **4**: e700.
- PALOMERO, T., M. L. SULIS, M. CORTINA, P. J. REAL, K. BARNES *et al.*, 2007 Mutational loss of PTEN induces resistance to NOTCH1 inhibition in T-cell leukemia. *Nature medicine* **13**: 1203-1210.
- POWELL, L. M., P. I. ZUR LAGE, D. R. PRENTICE, B. SENTHINATHAN and A. P. JARMAN, 2004 The proneural proteins Atonal and Scute regulate neural target genes through different E-box binding sites. *Molecular and cellular biology* **24**: 9517-9526.
- PROUDFOOT, L., J. R. KUSEL, H. V. SMITH, W. HARNETT, M. J. WORMS *et al.*, 1993 Rapid changes in the surface of parasitic nematodes during transition from pre- to post-parasitic forms. *Parasitology* **107 ( Pt 1)**: 107-117.
- QUACH, T. K., H. T. CHOU, K. WANG, G. Z. MILLEDGE and C. M. JOHNSON, 2013 Genome-wide microarray analysis reveals roles for the REF-1 family member HLH-29 in ferritin synthesis and peroxide stress response. *PloS one* **8**: e59719.
- RIESEN, M., I. FEYST, N. RATTANAVIROTKUL, M. EZCURRA, J. M. TULLET *et al.*, 2014 MDL-1, a growth- and tumor-suppressor, slows aging and prevents germline hyperplasia and hypertrophy in *C. elegans*. *Aging*.
- ROSS, J. M., A. K. KALIS, M. W. MURPHY and D. ZARKOWER, 2005 The DM domain protein MAB-3 promotes sex-specific neurogenesis in *C. elegans* by regulating bHLH proteins. *Dev Cell* **8**: 881-892.
- ROUAULT, J. P., P. E. KUWABARA, O. M. SINILNIKOVA, L. DURET, D. THIERRY-MIEG *et al.*, 1999 Regulation of dauer larva development in *Caenorhabditis elegans* by daf-18, a homologue of the tumour suppressor PTEN. *Curr Biol* **9**: 329-332.
- SANG, L., J. M. ROBERTS and H. A. COLLER, 2010 Hijacking HES1: how tumors co-opt the anti-differentiation strategies of quiescent cells. *Trends in molecular medicine* **16**: 17-26.
- SCHNABEL, R., and J. R. PRIESS, 1997 Specification of Cell Fates in the Early Embryo in *C. elegans II, 2nd edition*, edited by D. L. RIDDLE, T. BLUMENTHAL, B. J. MEYER and J. R. PRIESS. Cold Spring Harbor Laboratory Press, Cold Spring Harbor (NY).
- SOLARI, F., A. BOURBON-PIFFAUT, I. MASSE, B. PAYRASTRE, A. M. CHAN *et al.*, 2005 The human tumour suppressor PTEN regulates longevity and dauer formation in *Caenorhabditis elegans*. *Oncogene* **24**: 20-27.
- SONNEVILLE, R., M. QUERENET, A. CRAIG, A. GARTNER and J. J. BLOW, 2012 The dynamics of replication licensing in live *Caenorhabditis elegans* embryos. *The Journal of cell biology* **196**: 233-246.
- SZKLARCZYK, D., A. FRANCESCHINI, M. KUHN, M. SIMONOVIC, A. ROTH *et al.*, 2011 The STRING database in 2011: functional interaction networks of proteins, globally integrated and scored. *Nucleic acids research* **39**: D561-568.
- TISSENBAUM, H. A., J. HAWDON, M. PERREGAUX, P. HOTEZ, L. GUARENTE *et al.*, 2000 A common muscarinic pathway for diapause recovery in the distantly related nematode species *Caenorhabditis elegans* and *Ancylostoma caninum*. *Proc Natl Acad Sci U S A* **97**: 460-465.
- TOMITA, K., K. MORIYOSHI, S. NAKANISHI, F. GUILLEMOT and R. KAGEYAMA, 2000 Mammalian achaete-scute and atonal homologs regulate neuronal versus glial fate determination in the central nervous

- system. The EMBO journal **19**: 5460-5472.
- VAN DER VOET, M., M. A. LORSON, D. G. SRINIVASAN, K. L. BENNETT and S. VAN DEN HEUVEL, 2009 C. elegans mitotic cyclins have distinct as well as overlapping functions in chromosome segregation. Cell cycle **8**: 4091-4102.
- WANG, S. W., B. S. KIM, K. DING, H. WANG, D. SUN *et al.*, 2001 Requirement for math5 in the development of retinal ganglion cells. Genes & development **15**: 24-29.
- WARD, S., and J. S. CARREL, 1979 Fertilization and sperm competition in the nematode Caenorhabditis elegans. Developmental biology **73**: 304-321.
- WHITE, A., A. FEARON and C. M. JOHNSON, 2012 HLH-29 regulates ovulation in C. elegans by targeting genes in the inositol triphosphate signaling pathway. Biology Open **1**: 261 - 268.
- WONG, G. W., G. C. KNOWLES, T. W. MAK, A. A. FERRANDO and J. C. ZUNIGA-PFLUCKER, 2012 HES1 opposes a PTEN-dependent check on survival, differentiation, and proliferation of TCRbeta-selected mouse thymocytes. Blood **120**: 1439-1448.
- WRISCHNIK, L. A., and C. J. KENYON, 1997 The role of lin-22, a hairy/enhancer of split homolog, in patterning the peripheral nervous system of C. elegans. Development **124**: 2875-2888.
- XING, Y., A. LI, Z. BOROK, C. LI and P. MINOO, 2012 NOTCH1 is required for regeneration of Clara cells during repair of airway injury. Stem cells **30**: 946-955.

**Table 1. Validation of randomly selected HLH-25 targets by RT-qPCR**

WormBase ID	Sequence ID	Gene Name	log <sub>2</sub> FC (microarray)	log <sub>2</sub> FC (RT-qPCR)
WBGene00000230	F27C1.7	<i>atp-3</i>	1.14405	1.203510
WBGene00015102	B0280.5	<i>cpg-2</i>	1.29866	2.277368
WBGene00000913	T07A9.6	<i>daf-18*</i>	1.57550	1.181618
WBGene00001263	K04H4.1	<i>emb-9</i>	1.77821	0.688850
WBGene00010305	F59A2.5	F59A2.5*	-1.17632	-1.630390
WBGene00001394	W02A2.1	<i>fat-2*</i>	1.03562	1.718458
WBGene00014095	ZK829.4	<i>gdh-1*</i>	2.48027	1.338850
WBGene00001758	Y45G12C.2	<i>gst-10*</i>	1.36737	0.774000
WBGene00003022	ZK418.4	<i>lin-37</i>	1.58496	1.489140
WBGene00003037	JC8.8	<i>lin-54</i>	0.59567	0.425533
WBGene00003230	W02A2.7	<i>mex-5</i>	1.04264	0.574521
WBGene00003231	AH6.5	<i>mex-6</i>	1.11770	0.656000
WBGene00003242	C37C3.6	<i>mig-6</i>	1.71370	0.877350
WBGene00003473	K11G9.6	<i>mtl-1*</i>	-4.08804	-1.578000
WBGene00004078	F52E1.1	<i>pos-1</i>	1.91456	1.017858
WBGene00004302	K01G5.4	<i>ran-1*</i>	1.49570	0.989226
WBGene00004736	K11D9.2	<i>sca-1</i>	1.78660	1.270413
WBGene00004984	ZC404.8	<i>spn-4</i>	2.06005	0.947934
WBGene00009221	F28F8.2	<i>acs-2</i>	-1.71450	1.107159
WBGene00003421	F09E8.3	<i>msh-5</i>	1.70929	-1.120290
WBGene00011733	T12D8.5	T12D8.5	-3.24793	0.441060

\*target previously predicted by protein binding microarray (GROVE *et al.* 2009)

**Table 2. Hub Genes in the HLH-25 Network**

Wormbase ID	Sequence ID	Gene Name	Functional Summary <sup>^</sup>	GO Cluster Association*					
				ED	S	P	M	G	C
WBGene00000479	C07H6.5.2	<i>cgh-1</i>	ATP-dependent helicase; prevents apoptosis of developing embryos	X	X	X	X	X	
WBGene00000866	Y43E12A.1	<i>cyb-2.1</i>	Cyclin B family; required for oocyte maturation	X	X	X		X	X
WBGene00000868	T06E6.2a.2	<i>cyb-3</i>	G2/mitotic-specific, Cyclin B3	X	X	X			X
WBGene00000913	T07A9.6	<i>daf-18</i>	Phosphatase; negative regulator of insulin-like signaling	X			X	X	
WBGene00003155	C25D7.6.2	<i>mcm-3</i>	DNA replication licensing factor	X			X		X
WBGene00004239	Y45F10A.2.1	<i>puf-3</i>	RNA binding protein; required for cell cycle timing, spindle positioning, pronuclei formation	X	X				X

<sup>^</sup>Functional summaries are based on Wormbase annotations ([www.wormbase.org](http://www.wormbase.org))

\*ED, embryonic development ending in birth; S, sexual reproduction; P, nucleoside, proton transport; M, meiosis; G, regulation of growth; C, cell cycle



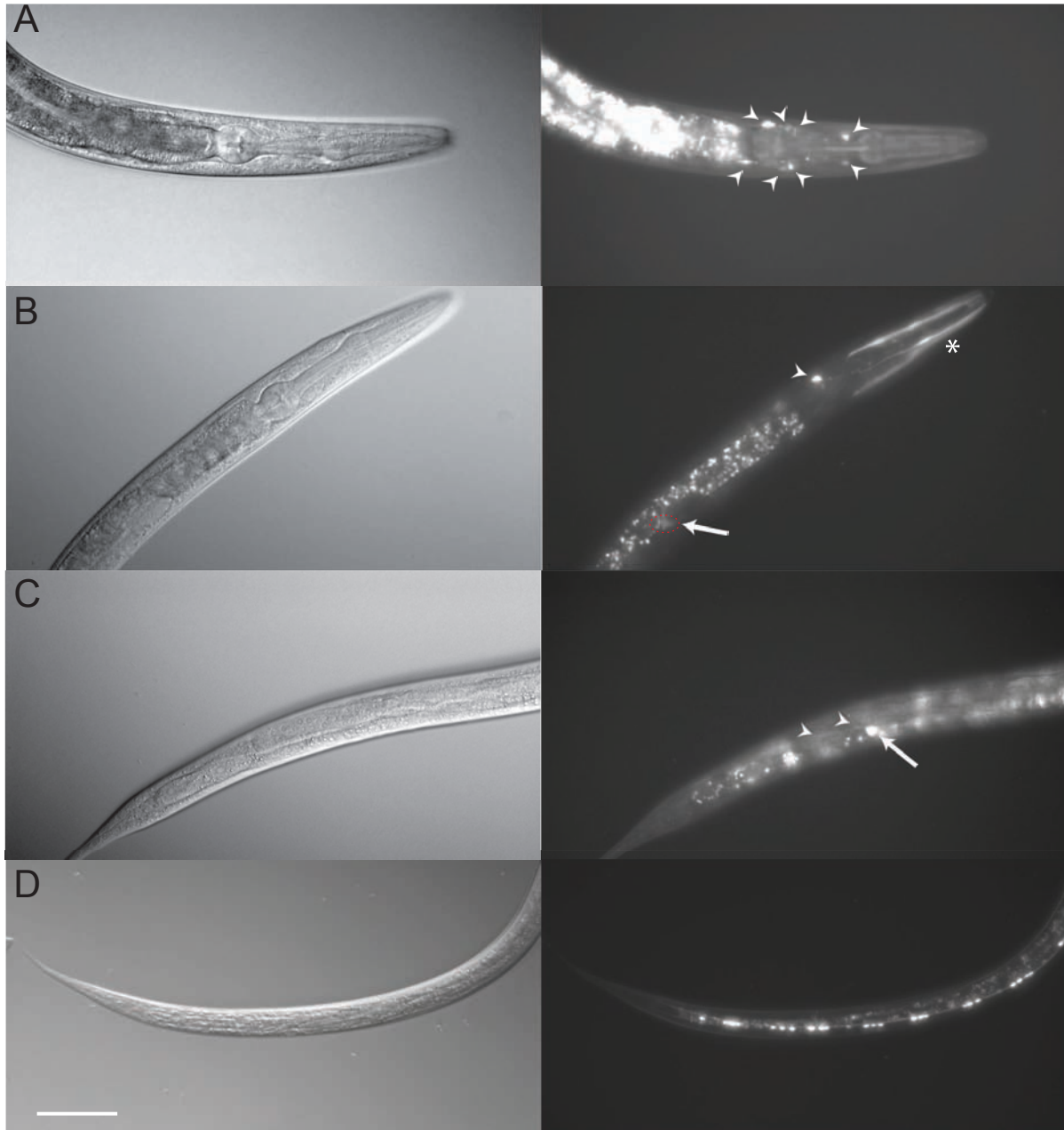
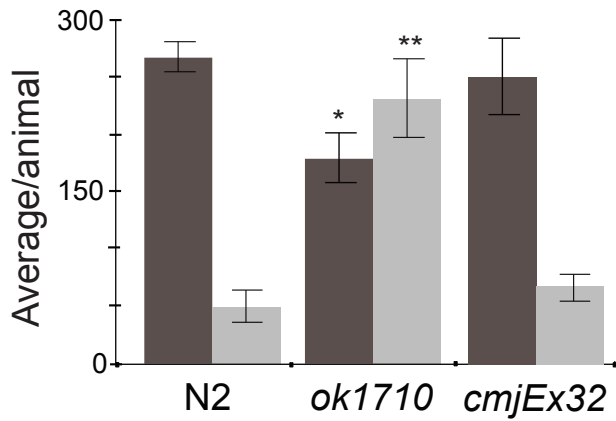


**Figure 1. Postembryonic expression of Phlh-25::GFP.** A-D) Nomarski images (left) accompanied by GFP fluorescent images (right). A) Expression of *cmjEx31* in multiple head neurons (arrowheads). This pattern was detected in animals at all stages, with a few additional neurons at dauer stage. B) L3 expression in distal tip cell (arrow, red dashed circle), unidentified head neuron (arrowhead) and head muscles (asterisk). C) L3 stage expression in PDE (arrow). Arrowheads indicate PDE processes. D) Dauer stage expression in ventral nerve cord neurons. In all images anterior is to the right, dorsal is up. Scale bar represents 50  $\mu$ m.

A



B

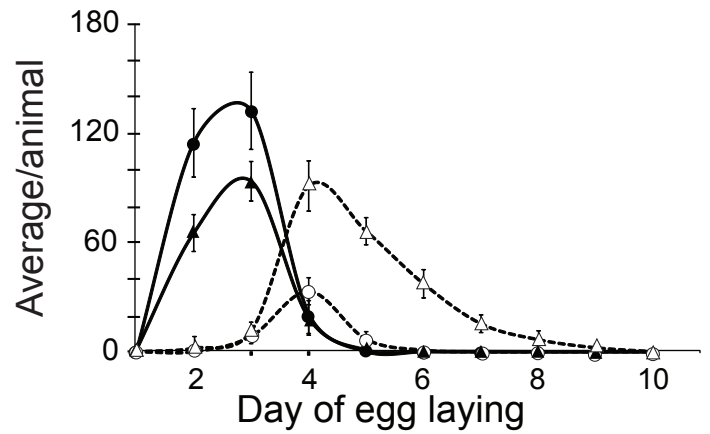


**Figure 2. Brood size and unfertilized oocytes *hlh-25(ok1710)* animals.** A) *hlh-25(ok1710)* animals have fewer live progeny and lay more unfertilized eggs than wild-type animals. Expression of the extrachromosomal array *cmjEx32*, which carries *hlh-25* genomic sequences, rescues this phenotype in *hlh-25(ok1710)* animals. Graph shows mean of total numbers of live progeny (dark bars) and unfertilized eggs (light bars) produced during the entire lifespans of wild-type ( $n = 7$ ), *hlh-25(ok1710)* ( $n = 12$ ), and *hlh-25(ok1710); cmjEx32* animals ( $n = 9$ ). \* P-value < 0.05, \*\*P-value < 0.005. B) Average numbers of live progeny (solid lines) and unfertilized eggs (dashed lines) produced per day of egg laying by the same *hlh-25(ok1710)* animals (triangles) and wild-type animals (circles) as

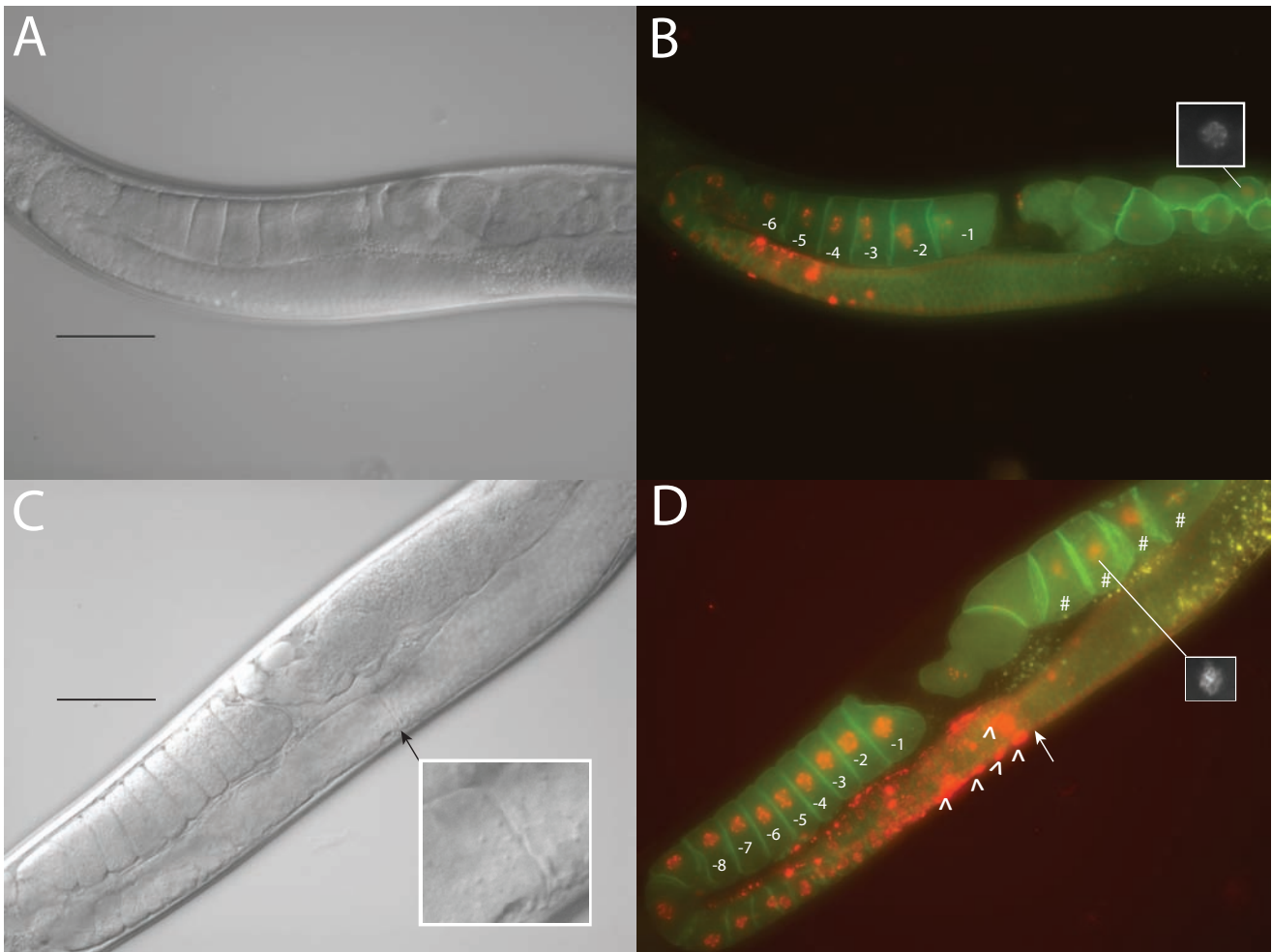


**Figure 3. Gonad and oocyte morphologies of *hlh-25(ok1710)* animals.** Nomarski (A, C) and merged fluorescent (B,D) images of representative gonad architecture and oocyte morphology in wild-type animals (A,B) as analyzed in a strain co-expressing a fluorescent chromosome marker (mCherry-Histone H2b) and a marker targeting GFP to the plasma membrane (PI4,5P2) (GREEN et al. 2011), (B). Representative gonad architecture and oocyte morphology in *hlh-25(ok1710)* animals (C,D). Phenotypes include increased oocyte number, distal gonad arm constriction (arrow), increased apoptosis (^), and arrested embryos in uterus (#). Insert in C) shows magnified view of distal gonad arm constriction. Inserts in B) and D) show embryonic nuclei. In all images, ventral is up, anterior is to the right, scale bar = 50  $\mu$ m.

A

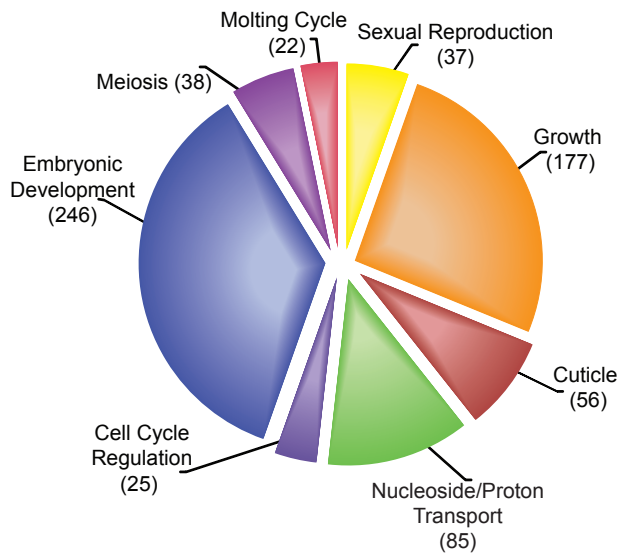
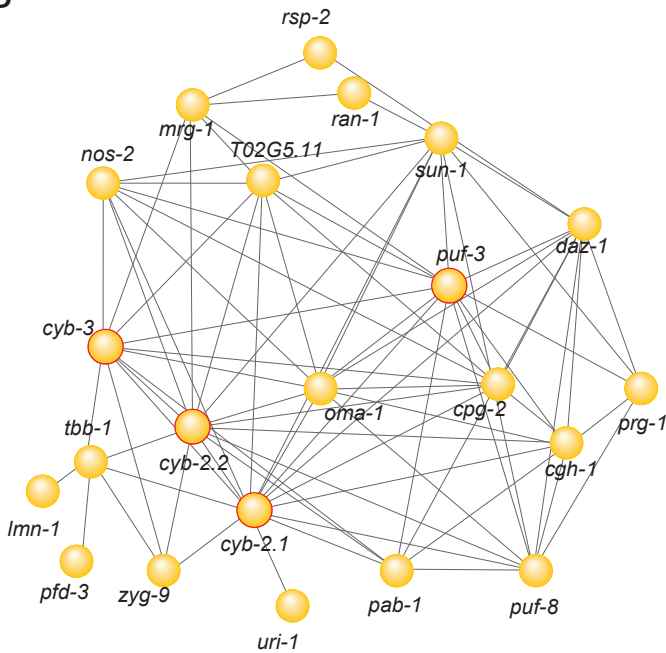
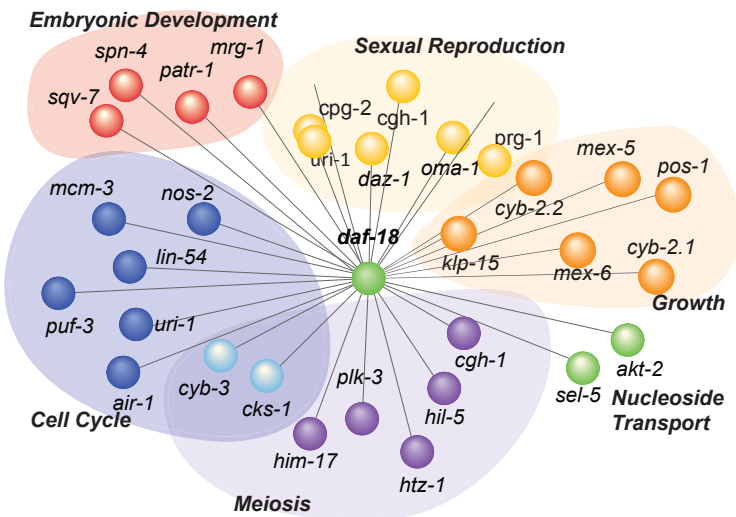


**Figure 4. Functional annotation of HLH-25 targets.** A) Distribution of HLH-25 targets into top eight GO clusters. B) Predicted and known interactions between genes in the ‘SEXUAL REPRODUCTION’ cluster. The hub genes *cgh-1*, *cyb-2.1*, *cyb-2.2*, *cyb-3*, and *puf-3* are outlined in red. The hub gene *daf-18* is not a part of the ‘SEXUAL REPRODUCTION’ cluster. C) Representative genes from the 62 HLH-25 targets that form predicted or known interactions with *daf-18*. All genes, except *daf-18*, clustered under “EMBRYONIC DEVELOPMENT ENDING IN BIRTH (EDB)” Most genes also clustered under at least one other top GO category, including “NUCLEOSIDE/NUCLEOTIDE TRANSPORT” (green ovals).

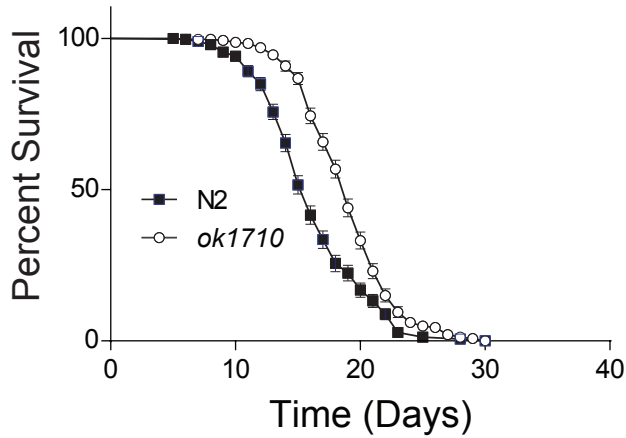
B



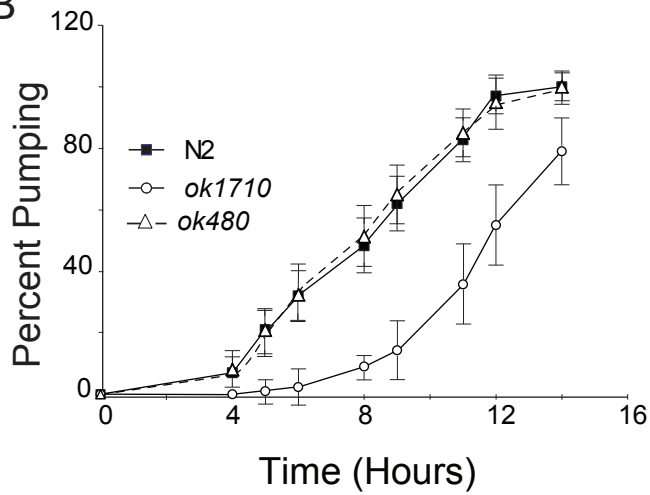
C



A



B



C

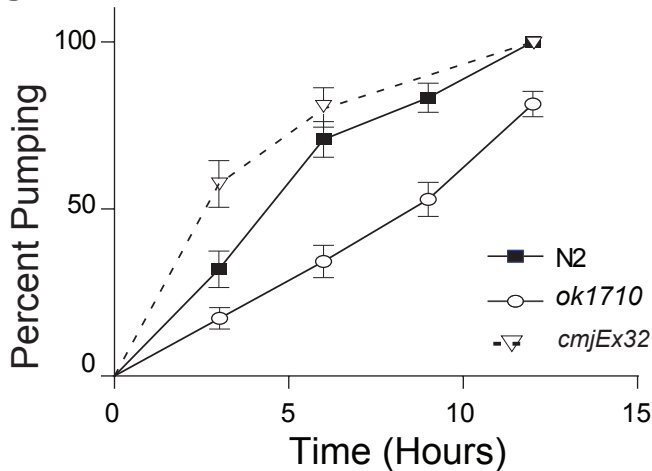


**Figure 5. HLH-25 regulates lifespan and dauer recovery.** A) *hlh-25(ok1710)* animals (n = 282) have longer than lifespans than wild-type animals (n = 264, P-value <0.0001). B) Representative experiment showing the percentage of animals with pharyngeal pumping during dauer recovery at 20°C. P-value <0.0001 and P-value = 0.938 when *hlh-25(ok1710)* animals and *daf-18(ok480)* animals, respectively, were compared to wild-type. C) Representative experiment showing the percentage of animals with pharyngeal pumping during dauer recovery at 20°C. P-value <0.0001 and P-value = 0.2771 when *hlh-25(ok1710)* and *hlh-25(ok1710);cmjEx32* animals, respectively, were compared to wild-type.